MEASUREMENT OF F_2 AT LOW Q^2 USING QED COMPTON SCATTERING AT HERA

V. LENDERMANN
DESY, Notkestr. 85, 22607 Hamburg, Germany
E-mail: victor@mail.desy.de

The proton structure function F_2 is measured in QED Compton scattering at HERA using data collected in 1997 by the H1 experiment. QED Compton events give access to the kinematic range of very low Q^2, down to $0.1\,\mathrm{GeV}^2$, and medium Bjorken x, a region which was not covered by inclusive DIS measurements at HERA. The results are in agreement with the measurements from fixed target experiments wherever they overlap.

1 Introduction

The *ep* scattering experiments at HERA have shown that the Q^2 evolution of the proton structure function $F_2(x, Q^2)$ is well described by perturbative Quantum Chromodynamics (pQCD) throughout a wide range in the Bjorken variable x and the negative four-momentum transfer squared, Q^2 [1–4]. However, at small Q^2 deviations from pQCD predictions are observed [4, 5], indicating the transition into a domain in which non-perturbative effects dominate and the data can only be described by phenomenological models.

In order to study this non-perturbative regime, F_2 has been measured at low Q^2, either employing special devices mounted close to the outgoing electron beam [5] or using "shifted vertex" data [6, 7]. In this paper preliminary results of a new measurement by H1 in this kinematic region are presented, which utilises *ep* data with wide angle hard photon radiation, so called QED Compton (QEDC) events.

2 QED Compton Scattering

Radiative processes in *ep* scattering, as depicted in fig. 1, may be split into three different classes [8, 9] with (i) the bremsstrahlung or Bethe-Heitler process corresponding to small masses of both the virtual electron and the virtual photon, (ii) the QED Compton process with a low virtual photon and a large

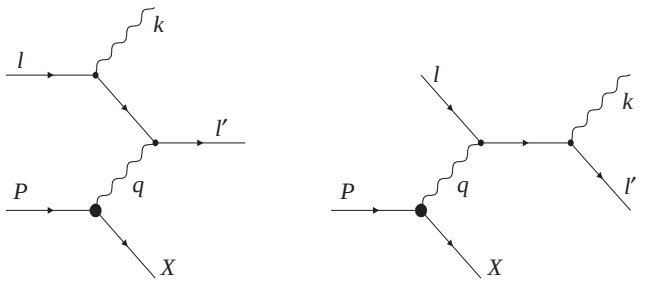

Figure 1: Lowest order Feynman diagrams for the *ep* scattering with photon emission from the electron line. Letters denote the particle four-momenta.

virtual electron mass and finally (iii) the radiative DIS process where the photon is collinear either with the incoming (Initial State Radiation, ISR) or the outgoing (Final State Radiation, FSR) electron. All three classes correspond to distinct experimental signatures. For the QEDC scattering process the final state topology is given by an azimuthal back-to-back configuration of the outgoing electron and photon detected under rather large scattering angles. In this configuration their transverse momenta balance such that very low values of the exchanged photon virtuality Q^2 are experimentally accessible.

At so low Q^2 three separate contributions have to be considered depending on the value of the invariant mass W of the hadronic final state:

1. Elastic scattering, for which the proton stays intact ($W = m_p$). This channel is well measured, and the cross section is given by the electric and magnetic form factors G_E and G_M;

2. Resonance production, where the total mass of the hadronic final state X lies in the range $m_p + m_\pi \lesssim W \lesssim 2\,\mathrm{GeV}$;

3. Continuum inelastic scattering at $W \gtrsim 2\,\mathrm{GeV}$. In this region the $\gamma^* p$ cross section is defined through the structure functions F_2 and F_L.

All the three channels are simulated by the COMPTON Monte Carlo event generator [8, 10]. The program also calculates higher order corrections for Initial State Radiation in the peaking approximation [11, 12]. However, as this generator was primarily written for an application in analyses of elastic QEDC events, in the original version a rather crude approach is employed to describe the resonance region and only simple scale invariant F_2 parameterisations are

used to model the continuum inelastic domain. Furthermore, no hadronisation of the final state X is performed.

Since this analysis aims at the investigation of inelastic QEDC events a new version of the COMPTON generator was developed [13] which includes detailed parameterisations for the resonance [14] and the continuum [15] regions. In addition, several packages for a complete simulation of the hadronic final state have been implemented into the program. For the present study the SOPHIA package [16] is used in the range of low Q^2 and low masses, W, of the hadronic final state, while the Quark Parton Model with subsequent Lund string fragmentation [17] is employed at high W and high Q^2.

3 Experimental Technique

The measurement is performed on $9.25\,\mathrm{pb}^{-1}$ of e^+p data with the centre-of-mass energy $\sqrt{s} = 301\,\mathrm{GeV}$, which were collected with the H1 detector at HERA in 1997.

The outgoing electron and photon in QEDC events are selected in the H1 detector [18] by requiring two energy depositions (clusters) in the electromagnetic part of the backward[1] lead-fibre calorimeter SpaCal [19]. The Backward Drift Chamber (BDC) [20] situated in front of the SpaCal is employed as a pre-shower detector to increase the precision of the cluster position measurement for electrons and converted photons. In events with the electron scattered in the inner part of the SpaCal, the Backward Silicon Tracker (BST) [21] is used to measure the electron polar angle and to reconstruct the interaction vertex position. In events in which the electron is scattered out of the BST acceptance, the Central Inner Proportional Chamber (CIP) [18] in conjunction with BDC and SpaCal is employed to determine the vertex coordinates. The hadronic final state is measured in the Liquid Argon Calorimeter (LAr) [18].

4 Background Processes

A prominent background to inelastic QEDC scattering is created by inclusive DIS events in which one particle from the hadronic final state (typically a π^0) fakes the outgoing photon producing a cluster in the electromagnetic SpaCal. Such events are modelled using the DJANGO MC generator [22]. At high y, where the hadronic final state particles lie mostly in the hemisphere of the

[1] The z axis of the right-handed coordinate system used by H1 is defined to lie along the direction of the incident proton beam and the origin to be at the nominal ep interaction vertex. The backward direction is thus defined through $z < 0$.

scattered electron and photon, this process dominates the QEDC signal making a clear QEDC event selection impossible. For this reason the measurement is restricted to relatively low y values: $y \lesssim 0.006$.

Another source of significant background is Deeply Virtual Compton Scattering (DVCS), in which the final state photon is radiated from the proton side. Elastic DVCS events were simulated by the TINTIN generator [23] and the cross section was normalised to the H1 results [24]. At present there is no theoretical prediction and no measurement for the inelastic DVCS cross section. The ratio of the inelastic to elastic scattering cross section was therefore estimated experimentally to be of a similar size as for diffractive vector meson electroproduction.

Further background sources considered are comparatively small, typically of the order $\lesssim 1\%$.

5 F_2 Measurement and Results

For the kinematic range in question, the reconstruction of the variables x and y cannot be performed using only the four-momenta of the outgoing electron and photon, as the resolution deteriorates with $1/y$ thus becoming inapplicable at low values of the inelasticity y. Therefore these variables were reconstructed using the Sigma method [25] which also deploys final state hadrons. Hence one of the main challenges for the analysis is a good understanding of the hadronic final state and the acceptance corrections in this region.

In order to extract the structure function F_2 the data sample is divided into subsamples corresponding to a grid in y and Q^2. The bin sizes are adapted to the resolution in the measured kinematic quantities such that purity and stability[2]in all bins shown are greater than 30%. Both the statistical and the systematic errors lie in the range $8 - 13\%$ making thus the total error to be $12 - 18\%$.

The F_2 values measured in QED Compton scattering are depicted in fig. 2 as a function of x at fixed Q^2 and compared to other HERA [5,26,27] and fixed target [28–30] data. The present analysis extends the kinematic range of HERA at very low Q^2 towards higher x values thus complementing standard inclusive and shifted vertex measurements. For inclusive DIS at nominal vertex position the outgoing electron is not detected in the H1 apparatus for such low values of Q^2 as it is scattered at small angles escaping through the beam pipe unseen. On the other hand shifted vertex data cannot extend the low Q^2 measurements to

[2]The purity (stability) is defined as the ratio of the number of simulated QEDC events originating from and reconstructed in a specific bin to the number of reconstructed (generated) events in the same bin.

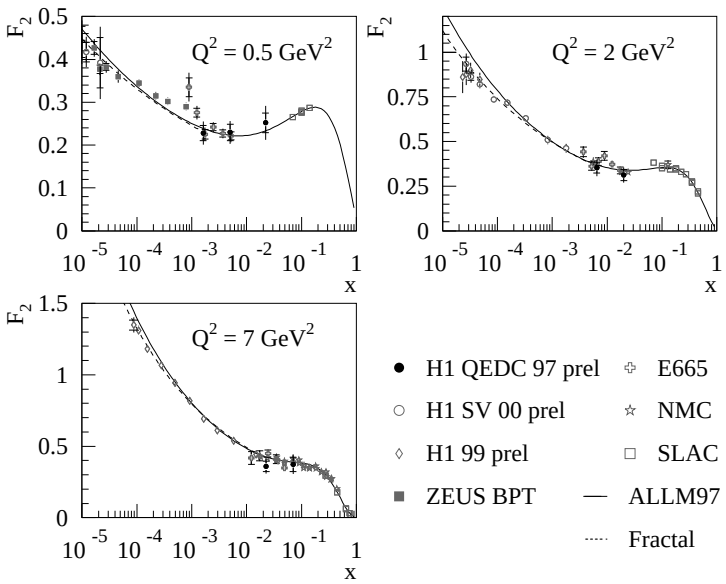

Figure 2: Results of F_2 measurement in QED Compton scattering (closed circles) compared with other measurements at HERA (closed squares [5], open diamonds [26] and open circles [27]) and fixed target experiments (open squares [28], open stars [29] and open crosses [30]). The solid line depicts the ALLM97 parameterisation [15], while the dashed line represents the Fractal fit [31], which is plotted in the range $y > 0.003$.

such high x due to stronger acceptance limitations in the forward region. The region covered mostly overlaps with the domain of fixed target experiments. A good agreement with their results is observed.

References

[1] C. Adloff *et al.* [H1 Collaboration], Eur. Phys. J. C **21** (2001) 33.

[2] S. Aid *et al.* [H1 Collaboration], Nucl. Phys. B **470** (1996) 3.

[3] S. Chekanov *et al.* [ZEUS Collaboration], Eur. Phys. J. C **21** (2001) 443.

[4] C. Adloff *et al.* [H1 Collaboration], Phys. Lett. B **393** (1997) 452.

[5] J. Breitweg *et al.* [ZEUS Collaboration], Phys. Lett. B **487** (2000) 53.

[6] M. Derrick *et al.* [ZEUS Collaboration], Z. Phys. C **69** (1996) 607.

[7] C. Adloff *et al.* [H1 Collaboration], Nucl. Phys. B **497** (1997) 3.

[8] A. Courau and P. Kessler, Phys. Rev. D **46** (1992) 117.

[9] T. Ahmed *et al.* [H1 Collaboration]: Z. Phys. C **66** (1995) 529.

[10] T. Carli, A. Courau, S. Kermiche and P. Kessler, in *Proceedings of the Workshop "Physics at HERA"*, 1992, Vol. 2, p. 902 and Vol. 3, p. 1468.

[11] E. Etim, G. Pancheri and B. Touschek, Nuovo Cim. B **51S10** (1967) 276.

[12] G. Pancheri, Nuovo Cim. B **60S10** (1969) 321.

[13] V. Lendermann, Doctoral Thesis, University of Dortmund, 2002.

[14] F. W. Brasse *et al.*, Nucl. Phys. B **110** (1976) 413.

[15] H. Abramowicz and A. Levy, DESY–97–251, hep–ph/9712415.

[16] A. Mücke *et al.*, Comput. Phys. Commun. **124** (2000) 290.

[17] T. Sjöstrand *et al.*, Comput. Phys. Commun. **135** (2001) 238.

[18] I. Abt *et al.* [H1 Collaboration], Nucl. Instrum. Meth. A **386** (1997) 310 and 348.

[19] R. D. Appuhn *et al.* [H1 SpaCal Group], Nucl. Instrum. Meth. A **374** (1996) 149, A **382** (1996) 395 and A **386** (1997) 397.

[20] B. Schwab, Doctoral Thesis, Ruprecht Karl University of Heidelberg, 1996.

[21] V. Arkadov, Doctoral Thesis, Humboldt University of Berlin, 2000.

[22] G. A. Schuler and H. Spiesberger, in *Proceedings of the Workshop "Physics at HERA"*, 1992, Vol. 3, p. 1419.

[23] R. Stamen, Doctoral Thesis, University of Dortmund, 2001.

[24] C. Adloff *et al.* [H1 Collaboration], Phys. Lett. B **517** (2001) 47.

[25] U. Bassler and G. Bernardi, Nucl. Instrum. Meth. A **361** (1995) 197.

[26] H1 Collaboration, contributed paper to EPS 2001, Budapest;
Abstract **799**, Parallel Session **1**.

[27] H1 Collaboration, contributed paper to EPS 2003, Aachen;
Abstract **082**, Parallel Session **4**.

[28] L. W. Whitlow *et al.*, Phys. Lett. B **282** (1992) 475.

[29] M. Arneodo *et al.* [New Muon Collaboration], Nucl. Phys. B **483** (1997) 3.

[30] M. R. Adams *et al.* [E665 Collaboration], Phys. Rev. D **54** (1996) 3006.

[31] T. Laštovička, Eur. Phys. J. C **24** (2002) 529.